⌘ *Author's Choice*

THE JOURNAL OF BIOLOGICAL CHEMISTRY VOL. 287, NO. 27, pp. 22533–22548, June 29, 2012
© 2012 by The American Society for Biochemistry and Molecular Biology, Inc. Published in the U.S.A.

58-kDa Microspherule Protein (MSP58) Is Novel Brahma-related Gene 1 (BRG1)-associated Protein That Modulates p53/p21 Senescence Pathway*[S]

Received for publication, December 18, 2011, and in revised form, May 4, 2012 Published, JBC Papers in Press, May 4, 2012, DOI 10.1074/jbc.M111.335331

Che-Chia Hsu,[a] Yi-Chao Lee,[b] Shiu-Hwa Yeh,[c1] Chang-Han Chen,[d1] Chih-Ching Wu,[e] Tsui-Ying Wang,[f] Yu-Nong Chen,[f] Liang-Yi Hung,[a] Yao-Wen Liu,[g] Han-Ku Chen,[h] Yi-Ting Hsiao,[c] Wei-Sheng Wang,[i] Jen-Hui Tsou,[a] Yi-Huan Tsou,[f] Mei-Hsiang Wu,[a] Wen-Chang Chang,[f,j,k,l2] and Ding-Yen Lin[a,f,j,k3]

From the [a]Institute of Bioinformatics and Biosignal Transduction, College of Bioscience and Biotechnology, [f]Department of Pharmacology, College of Medicine, [j]Center for Gene Regulation and Signal Transduction Research, and [k]Infectious Diseases and Signaling Research Center, National Cheng Kung University, Tainan 70101, Taiwan, [l]Graduate Institute of Medical Sciences, College of Medicine and [b]Program for Neural Regenerative Medicine, College of Medical Science and Technology, Taipei Medical University, Taipei 11031, Taiwan, [c]Institute of Biotechnology and Pharmaceutical Research, National Health Research Institutes, Miaoli 35053, Taiwan, [d]Center for Translational Research in Biomedical Sciences and [i]Department of Otolaryngology, Kaohsiung Chang Gung Memorial Hospital, Kaohsiung 833, Taiwan, [e]Department of Medical Biotechnology and Laboratory Science, College of Medicine, Chang Gung University, Taoyuan 333, Taiwan, [g]Department of Pathology, Kuo General Hospital, Tainan 700, Taiwan, and [h]Department of Pathology, Fooyin University Hospital, Pingtung 928, Taiwan

Background: The nucleolar MSP58 protein is a candidate oncogene implicated in cellular transformation.
Results: MSP58 is associated with BRG1 and induces cellular senescence through the p53/p21 pathway.
Conclusion: MSP58 has both tumor-suppressing and -promoting functions.
Significance: This work reveals a novel role for MSP58 in cellular senescence and suggests that MSP58 may have further prognostic and therapeutic implications.

The nucleolar 58-kDa microspherule protein (MSP58) protein is a candidate oncogene implicated in modulating cellular proliferation and malignant transformation. In this study, we show that knocking down MSP58 expression caused aneuploidy and led to apoptosis, whereas ectopic expression of MSP58 regulated cell proliferation in a context-dependent manner. Specifically, ectopic expression of MSP58 in normal human IMR90 and Hs68 diploid fibroblasts, the H184B5F5/M10 mammary epithelial cell line, HT1080 fibrosarcoma cells, primary mouse embryonic fibroblasts, and immortalized NIH3T3 fibroblasts resulted in induction of premature senescence, an enlarged and flattened cellular morphology, and increased senescence-associated β-galactosidase activity. MSP58-driven senescence was strictly dependent on the presence of functional p53 as revealed by the fact that normal cells with p53 knockdown by specific shRNA or cells with a mutated or functionally impaired p53 pathway were effective in bypassing MSP58-induced senescence. At least two senescence mechanisms are induced by MSP58. First, MSP58 activates the DNA damage response and p53/p21 signaling pathways. Second, MSP58, p53, and the SWI/SNF chromatin-remodeling subunit Brahma-related gene 1 (BRG1) form a ternary complex on the p21 promoter and collaborate to activate p21. Additionally, MSP58 protein levels increased in cells undergoing replicative senescence and stress-induced senescence. Notably, the results of analyzing expression levels of MSP58 between tumors and matched normal tissues showed significant changes (both up- and down-regulation) in its expression in various types of tumors. Our findings highlight new aspects of MSP58 in modulating cellular senescence and suggest that MSP58 has both oncogenic and tumor-suppressive properties.

Senescence is irreversible proliferative arrest that was first recognized by Hayflick and Moorhead (1) decades ago as a process that prevents normal fibroblasts from indefinitely dividing in culture. This "replicative senescence" was revealed to be tightly linked to telomere attrition (2–4) and is related to the *in vivo* aging of organisms (5). Subsequently, stressful stimuli, such as DNA damage, oxidative stress, and oncogene activation, were observed to cause stress-induced premature senescence in a telomere-independent manner (6–8). Cells entering senescence undergo permanent cell cycle arrest with a set of metabolic and morphological changes, such as adopting an enlarged and flattened cell shape, displaying a high frequency of nuclear abnormalities, expressing senescence-associated β-ga-

* This work was supported by National Science Council of Taiwan Grants NSC96-2320-B-006-011, NSC96-2320-B-006-049-MY2, and NSC98-2320-B-006-035-MY3) and National Cheng Kung University Landmark Grant C015 (to D.-Y. L.).
⌘ *Author's Choice*—Final version full access.
[S] This article contains supplemental Experimental Procedures, Figs. S1–S4, and Table S1.
[1] Both authors contributed equally to this work.
[2] To whom correspondence may be addressed: Graduate Inst. of Medical Sciences, College of Medicine, Taipei Medical University, Taipei 11031, Taiwan. E-mail: wcchang@mail.ncku.edu.tw.
[3] To whom correspondence may be addressed: Inst. of Bioinformatics and Biosignal Transduction, College of Bioscience and Biotechnology, National Cheng Kung University, Tainan 70101, Taiwan. Tel.: 886-6-2757575 (ext. 31207); Fax: 886-6-2083663; E-mail: lindy@mail.ncku.edu.tw.

lactosidase (SA-β-gal),[4] and showing altered gene expressions (9–11). The p53/p21 and Rb/p16 axes are two major tumor suppression pathways implicated in cellular senescence (6, 8, 12). Activation of p53 transactivates p21 and leads to the subsequent accumulation of underphosphorylated Rb (13, 14). Rb/p16 links senescence-associated heterochromatin focus formation and cell cycle gene silencing (15, 16).

Activated in the early stages of tumorigenesis, cellular senescence was demonstrated to function as a potent tumor suppressor that prevents malignant transformation. This suggests that escape from senescence leads to cell progression toward malignancy (17, 18). Therefore, discovering the reason a cell with genetic abnormalities or experiencing different stresses enters a senescent state and identifying the critical molecular events that might counteract this phenomenon appear to be necessary steps toward enhancing our understanding of tumor development. Acquiring greater knowledge of the pathways that modulate senescence can provide a basis for the development of more effective cancer treatments.

Previous studies identified the 58-kDa microspherule protein (MSP58), also known as microspherule protein 1, as an interacting partner of the proliferation-related nucleolar protein p120, a component of the nucleosome-remodeling and deacetylase complex; Mi-2β; and transcription factors Daxx, STRA13, and Nrf1 (19–23). Data from a recent study showed that *Drosophila* MCRS2 is co-purified with RNA polymerase II complexes and is required for normal levels of cyclin gene expression (24). Those findings imply that MSP58 proteins are crucial for transcriptional regulation in nuclei and nucleoli. In a separate line of evidence, p78, an isoform of MSP58, was found to interact and colocalize with the Nde1, Su48, and δ-interacting protein A centrosomal proteins and was implicated as having a role in centrosome dynamics (25, 26). Notably, MSP58 and TOJ3, a quail homologue of MSP58, behave as oncogenes in fibroblast transformation assays, whereas the tumor suppressor phosphatase and tensin homologue (PTEN) suppresses the transforming activity of MSP58 (27, 28). The role of MSP58 in regulating cell proliferation was further substantiated by the finding that RNAi-mediated inhibition of MSP58 reduced the growth of glioma and colorectal cancer cells (29, 30). In addition, an isoform of human MSP58, MCRS2, was involved in telomere shortening by associating with the telomerase-inhibitory protein, liver-related putative tumor suppressor/PIN2-interacting protein 1, and the catalytic telomerase subunit, human telomerase reverse transcriptase (31).

We previously reported that MSP58 can relieve the transcriptional repressor activity of Daxx through a nucleolar sequestration mechanism (20). In the current study, we further delineated the growth-regulatory role of MSP58 in several human cancerous and normal cells, demonstrated its impact on cellular senescence, and determined the underlying molecular basis of this phenomenon. We also detected the MSP58 expression profile in a broad range of normal and malignant human tissues. The results revealed links among MSP58, p53, and cellular senescence in human tumor and normal cells.

EXPERIMENTAL PROCEDURES

Plasmids and Antibodies—The mammalian vector for expression of FLAG-tagged MSP58 was described previously (20). A polymerase chain reaction (PCR) fragment encoding the full length (amino acids 1–462) of human MSP58 was in-frame subcloned into the pBTM116 vector with the LexA domain to generate the LexA-MSP58 bait. The PCR product was also cloned into the pEGFP-C2 vector (BD Biosciences Clontech) and further subcloned into the AgeI and BamHI sites of the pQCXIP retroviral vector (BD Biosciences Clontech) to generate pQCXIP-GFP-MSP58. pBJ5-HA-BRG1 was a gift from Drs. Stephen P. Goff (Howard Hughes Medical Institute, Columbia University, New York, NY) and Weei-Chin Lin (Departments of Medicine and Molecular and Cellular Biology, Baylor College of Medicine, Houston, TX). pGal-AD-BRG1 deletion mutants were engineered by subcloning PCR-amplified BRG1 fragments into the yeast vector pACT2, which expresses the Gal4 activation domain (BD Biosciences Clontech). The luciferase reporter plasmids pGL2-(−536) and pGL2-(−536) mut. driven by a wild-type (WT) and deletion mutant of E2F-responsive promoter sequences from the mouse B-*myb* gene as described (32) were a gift from Dr. Roger J. Watson (Ludwig Institute for Cancer Research, St. Mary's, Campus, London, UK). The p21 (CDKN1A) promoter-luciferase reporters including WT and p53-binding site mutants (p21-WT, p21-sm, and p21-dm) (33) were a gift from Dr. Axel H. Schönthal (University of Southern California, Los Angeles, CA) and were obtained from Dr. Shih-Ming Huang (National Defense Medical Center, Taipei, Taiwan). pcDNA3-HA-p53 was constructed by subcloning a PCR fragment of full-length p53 from pCMV-p53WT (BD Biosciences Clontech) into the pcDNA3-HA vector (Invitrogen). The pSUPER vector and its derivatives expressing small interfering (si) RNAs of human MSP58, ATM, p21, and BRG1 were constructed according to instructions from OligoEngine (Seattle, WA). The 19-nucleotide target sequences for siMSP58 were si-3 (5′-GAAGAAGAAGGTATCCAAA-3′) and si-5 (5′-CAAGGTGTCATCAAGCTGA-3′). ATM, p21, and BRG1 were knocked down as reported previously using the pSUPER system: siATM (34), 5′-ACTGTAAAGCTGCAATGAA-3′; sip21 (35), 5′-GACCATGTGGACCTGTCAC-3′; and siBRG1 (36), 5′-GGCAGAAGCACCAGGAATA-3′. As controls, we used the firefly luciferase-targeted oligonucleotide 5′-CTGACGCGGAATACTTCGA-3′. Lentivirus production and infection with short hairpin (sh) RNA targeting p53 were expressed from the pLKO TRC017 hairpin vector, which harbors an expression cassette for a neomycin resistance gene driven by the human phosphoglycerate kinase promoter. The shp53 sequence used was 5′-CACCATCCACTACAACTACAT-3′; pLKO.1-shLuc (TRCN0000072243; shLuc) was used

[4] The abbreviations used are: SA-β-gal, senescence-associated β-galactosidase; ATM, ataxia telangiectasia mutated; ATR, ATM- and Rad3-related; Chk, cell cycle checkpoint kinase; Daxx, Fas death domain-associated protein; Nde1, nudE nuclear distribution gene E homolog 1; Nrf1, nuclear factor-erythroid 2 p45 subunit-related factor 1; Rb, retinoblastoma protein; STRA13, stimulated by retinoic acid 13; TOJ3, target of Jun 3; X-Gal, 5-bromo-4-chloro-3-indolyl-β-D-galactopyranoside; MSP58, 58-kDa microspherule protein; BRG1, Brahma-related gene 1; PTEN, phosphatase and tensin homologue; MEF, mouse embryonic fibroblast; qPCR, quantitative PCR; IHC, immunohistochemical; γ-H2AX, phosphorylated histone H2AX; MOF, males absent on first; pRb, phosphorylated Rb; NuRD, nucleosome remodeling and deacetylase.

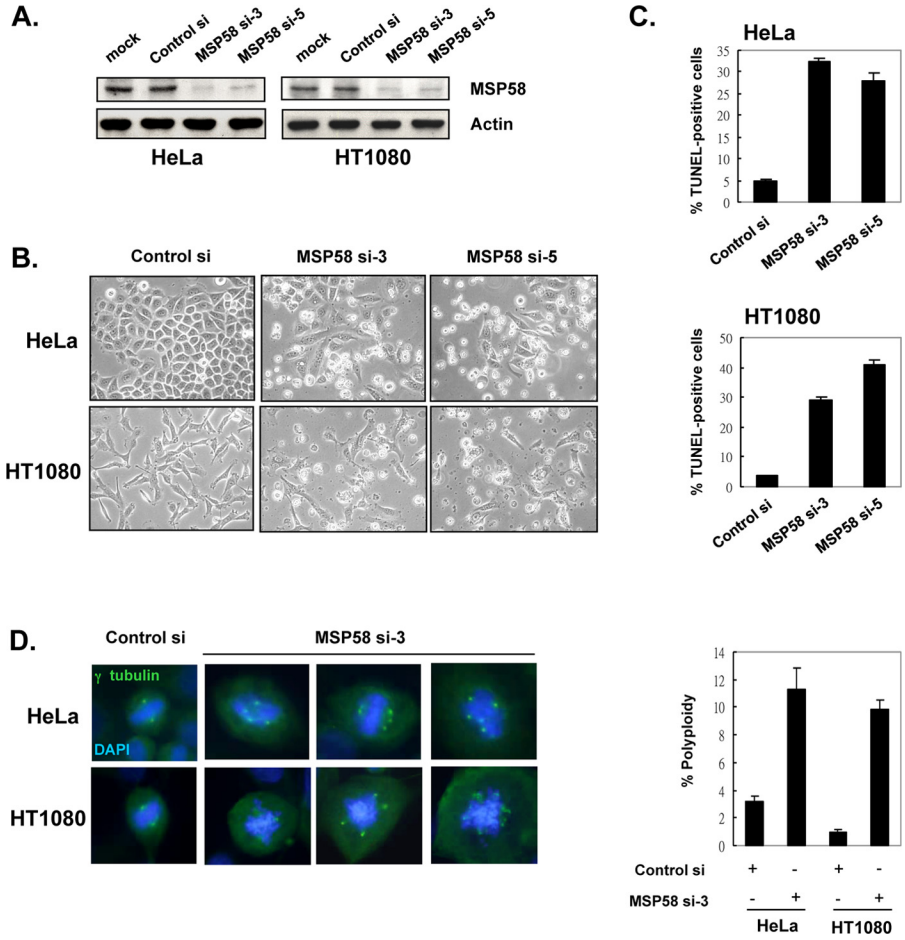

FIGURE 1. **MSP58 silencing causes apoptosis and aneuploidy.** *A*, HeLa and HT1080 cells were transiently transfected with a pSUPER empty vector (*mock*), negative control (*Control si*), or pSUPER-siMSP58 (MSP58 si-3 and MSP58 si-5) vector and harvested 72 h later for an immunoblot analysis of MSP58 expression using actin as the control. These transfected cells were also subjected to a microscopic analysis (*B*), TUNEL assay (*C*), and immunofluorescence analysis (*D*) by staining with an anti-γ-tubulin antibody and DAPI. *Columns*, mean of three independent experiments (*C* and *D*); *bars*, S.D. *D*, cells with multipolar, enlarged polyploidy were counted ($n = 250$).

as a control. These vectors were obtained from the The RNAi Consortium (TRC) library (National RNAi Core Facility, Academia Sinica, Taipei, Taiwan). Polyclonal antibodies raised in rabbits immunized with a synthetic peptide, MDKDSQGLLD, corresponding to amino acids 1–10 of human MSP58 were obtained from AgeneMax (Taipei, Taiwan). The following commercial antibodies were used in this study: FLAG (M2; Sigma), HA (HA.11; Babco/Covance, Berkley, CA), actin (clone AC-74; Sigma), p53 (BP53-12; Upstate Biotechnology, Lake Placid, NY), p21 (Upstate Biotechnology), cyclin B1 (Upstate Biotechnology), cyclin D (Upstate Biotechnology), cyclin E (Upstate Biotechnology), cyclin A (BF683; Cell Signaling Technology, Beverly, MA), cyclin E2 (Cell Signaling Technology), BRG1 (3G4; Upstate Biotechnology), ATM (2C1; GeneTex, San Antonio, TX), acetyl-p53Lys^{382} (Cell Signaling Technology), and green fluorescent protein (GFP; BD Biosciences Clontech). The Rb[4H1] monoclonal antibody (mAb) and phosphospecific pRbs (pRbSer(P)^{780}, pRbSer(P)$^{870/811}$, and pRbSer(P)^{795}) were from the PhosphoPlus Rb antibody kit (Cell Signaling Technology). Phospho-ATRSer^{428}, phospho-ATMSer^{1981}, phospho-Chk1Ser^{296}, phospho-Chk2Thr^{68}, phospho-histone H2A.XSer^{139}, and phospho-p53Ser^{15} antibodies were from the DNA Damage Antibody Sampler kit (Cell Signaling Technology).

Cell Culture—The normal human mammary epithelial cell line H184B5F5/M10 was purchased from the Bioresource Collection and Research Center (Hsinchu, Taiwan). All other cell lines were obtained from the American Type Culture Collection (Manassas, VA). Mouse embryonic fibroblasts (MEFs) from WT (p53$^{+/+}$) and p53-null (p53$^{-/-}$) mice were generously provided by Dr. Fung-Fang Wang (National Yang Ming University, Taipei, Taiwan). HeLa, SW-13, Hs68, NIH3T3, p53$^{+/+}$, and p53$^{-/-}$ MEF cells were cultured in Dulbecco's modified Eagle's medium (DMEM; Invitrogen) supplemented with 10% fetal bovine serum (FBS). HT1080, IMR90, and H184B5F5/M10 cells were maintained in minimum essential medium (Invitrogen) with 10% FBS. Saos-2 cells were maintained in McCoy's 5A medium (Sigma) with 15% FBS. All cells were maintained at 37 °C under a 5% CO_2 atmosphere.

Transient, Stable Transfection and Retroviral Transduction—Plasmids were transfected using FuGENE 6 reagent (Roche Applied Science). For stable transfection, cells were selected with either 400 μg/ml Geneticin (G418) or 2 μg/ml puromycin. To generate retrovirus- and lentivirus-producing cell lines,

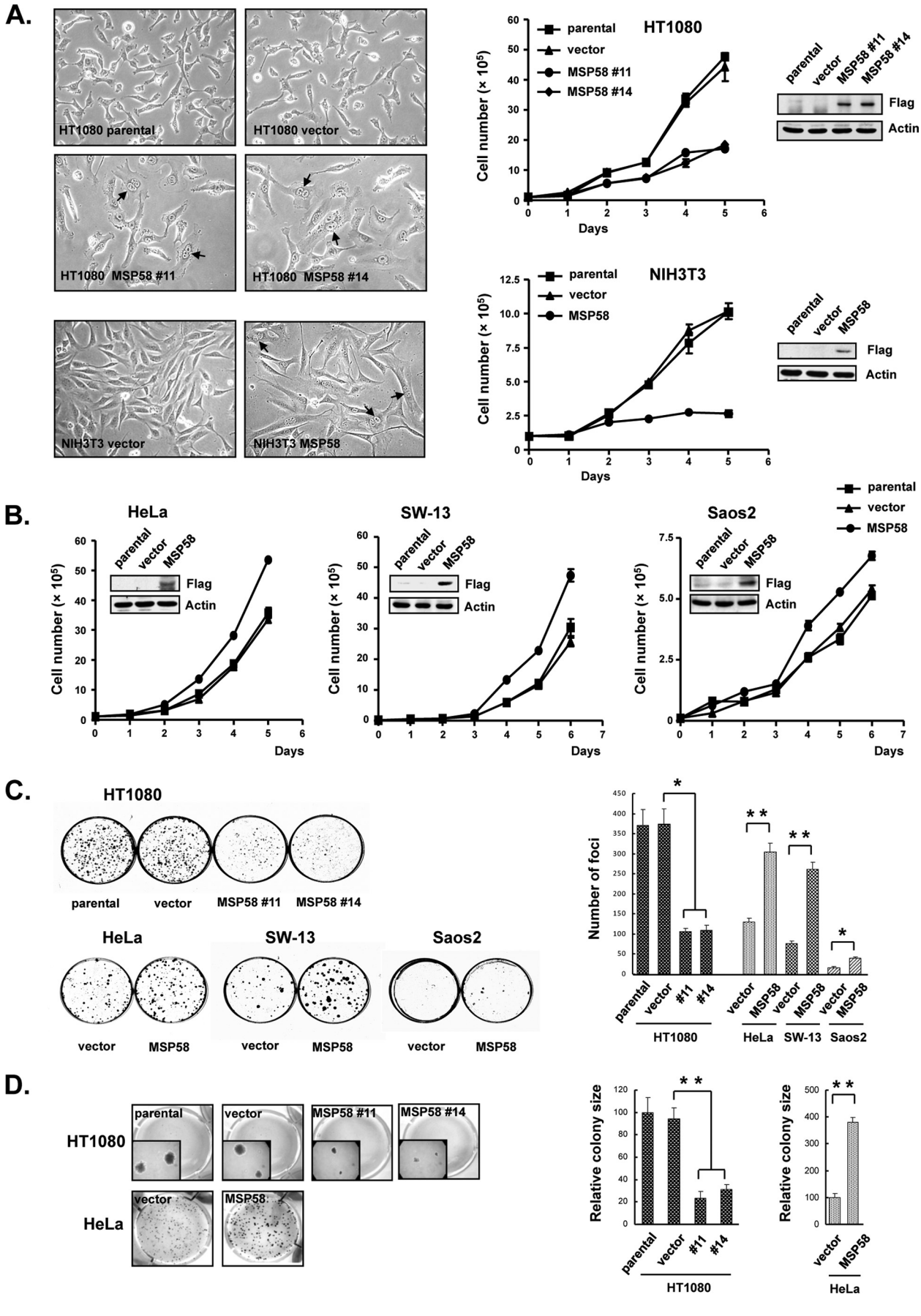
A.
HT1080 parental
HT1080 vector
HT1080 MSP58 #11
HT1080 MSP58 #14
NIH3T3 vector
NIH3T3 MSP58
HT1080
parental
vector
MSP58 #11
MSP58 #14
Cell number (× 10⁵)
Days
Flag
Actin
NIH3T3
MSP58
B.
HeLa
SW-13
Saos2
C.
HT1080
HeLa
SW-13
Saos2
parental
vector
MSP58 #11
MSP58 #14
MSP58
Number of foci
D.
Relative colony size

Lipofectamine 2000 (Invitrogen) was used to transfect 293T cells with a pQCXIP-GFP control, pQCXIP-GFP-MSP58 expression vector, or shRNA lentiviral vector; a murine leukemia virus Gag-Pol packaging vector; and the vesicular stomatitis virus envelope glycoprotein expression vector. Supernatants were collected 48 h post-transfection, filtered (0.45 μm), and immediately used to infect cells. After viral infection, cells were treated with 400 μg/ml Geneticin (G418) and/or puromycin (1.25 μg/ml) for selection. Neomycin- and/or puromycin-resistant cells were pooled for subsequent analysis.

Growth Curves, Focus Formation Assays, and Soft Agar Assays—The growth rate of cells was monitored by seeding 2×10^5 cells in 60-mm dishes containing 5% FBS. Samples were taken daily and counted using a hemocytometer. For the focus formation assay, cells were plated at a low density onto 100-mm dishes, and the medium was changed every 3 days. After 2 weeks, the number of colonies was counted using the Sigmascan software program after staining with 2% methylene blue. For the soft agar assay, 2000 cells were plated in 1 ml of complete growth medium containing 0.3% agarose and overlaid with 1.5 ml of 0.6% agarose. Cells were fed weekly. After 2–3 weeks, cells were stained with 0.05% crystal violet.

Cell Cycle and Apoptosis Assays—Cells transfected with the indicated plasmids were harvested, fixed, stained with propidium iodide, and analyzed by flow cytometry (BD Biosciences FACSCalibur flow cytometer). A terminal deoxynucleotidyltransferase-mediated dUTP nick end labeling (TUNEL) assay was performed using an APO-DIRECT ™ kit (BD Biosciences).

Analysis of Senescence—SA-β-gal staining was performed using a Senescence Detection kit (Cell Signaling Technology).

Western Blot, Coimmunoprecipitation, Immunofluorescence, Luciferase Assays, and Real Time Quantitative PCR (qPCR)—Western blot, coimmunoprecipitation, immunofluorescence, luciferase assays, and real time qPCR were performed as described previously (37). Nuclear extracts were prepared (38) for the endogenous coimmunoprecipitation experiments. A real time qPCR was performed using the SYBR Advantage qPCR Premix (Invitrogen). PCRs were then performed using the following conditions for 40 cycles: 95 °C for 15 s, 60 °C for 15 s, and 72 °C for 20 s. The following primer pairs were used: p21, forward (5′-ATGTGGACCTGTCACTGTCTTG) and reverse (5′-CGTTTGGAGTGGTAGAAATCTG); β-actin, forward (5′-ACTGGGACGACATGGAGAAG-3′) and reverse (5′-GGTACGACCAGAGGCATACAG-3′). The real time qPCR analysis was performed using a LightCycler instrument (Roche Applied Science). Relative transcript amounts of the p21 gene, calculated using standard curves of serial cDNA dilutions, were normalized to β-actin.

Chromatin Immunoprecipitation (ChIP)—ChIP and re-ChIP assays were performed as described previously (37). Briefly, sheared chromatin fragments were immunoprecipitated with antibodies specific to FLAG, BRG1, p53, or control immunoglobulin G (IgG) at 4 °C overnight. After dissociating the DNAs from the immunoprecipitated chromatin, the DNAs underwent PCR amplification. The two sequences containing p53-binding sites at −1688/−1335 and −2440/−2195 (respectively named numbers 1 and 2), and the sequence without the p53-binding site at −3558/−3141 (named number 3) were amplified. The following sets of primers were used: number 1, forward (5′-GAAATGCCTGAAAGCAGAGG) and reverse (5′-GCTCAGAGTCTGGAAATCTC); number 2, forward (5′-TGGGCTTTCCACCTTTCACCATTCC) and reverse (5′-CATCCCCTTCCTCACCTGAAAACAG); and number 3, forward (5′-GACATAGCAGGTGTGATGACC) and reverse (5′-GTATTCAGGTGGCTGAGGTG).

Yeast Two-hybrid Assay—Yeast two-hybrid screening and analysis were performed as described previously (20).

Matching Normal/Tumor Expression Array and Tissue Immunohistochemical (IHC) Staining—To analyze MSP58 messenger (m) RNA expressions between normal and tumor tissues, a dot-blot assay was purchased (Cancer Profiling Array II, BD Bioscience Clontech). Full-length ^{32}P-labeled human MSP58 cDNA was used for hybridization, and the radioactivity of each dot was visualized and quantitated using a phosphorimaging system (Fujifilm BAS 2500). The membrane was stripped and reprobed with a ubiquitin probe to normalize each signal. IHC staining was performed on US Biomax (Rockville, MD) tissue arrays (catalogue number BCN962) for MSP58. Clinical and pathologic information for individual cancer samples was provided by the array manufacturer. IHC staining was performed as described previously (39). Staining results were reviewed and scored by two pathologists (Y.-W. Liu and H.-K. Chen) blinded to each other's scoring.

Statistical Analysis—Statistical comparisons were performed using a two-tailed Student's *t* test. *p* values were calculated using the GraphPad Prism software version 3.03 package (GraphPad Software, San Diego, CA).

RESULTS

MSP58 Knockdown Cells Undergo Apoptosis—Initially, we generated and characterized polyclonal antibodies against MSP58. A 58-kDa band corresponding to MSP58 was readily detected by Western blotting (supplemental Fig. S1A). The main localization of MSP58 was consistently in nuclei and microspherule speckles of nucleoli with faint cytoplasmic staining (supplemental Fig. S1B). The data indicated that our antibody had high specificity and sensitivity for detecting the human MSP58 protein. To clarify the biological significance of MSP58 expression in cancer, we designed several shRNA constructs targeted to the MSP58 coding region (supplemental Experimental Procedures). The effectiveness of these shRNAs was initially examined through their transient cotransfection with the FLAG-MSP58 construct in 293T cells of which MSP58

FIGURE 2. **MSP58 modulates proliferation rate in cell context-dependent manner.** *A*, phase-contrast images and growth curves of HT1080 and NIH3T3 parental and/or vector and stably MSP58-overexpressing cells. Images are all at the same magnification (200×). *Arrows*, binucleated cells; *points*, mean value from three independent experiments, each run in triplicate; *bars*, S.D. MSP58 expression was analyzed using immunoblotting. *B*, growth curves (as in *A*) of HeLa, SW-13, and Saos-2 parental; stable control (*vector*); and MSP58-overexpressing cells. *C*, focus formation assays. Data represent the average number of foci ±S.D. from three independent experiments performed in triplicate. *, $p < 0.05$; **, $p < 0.01$. *D*, soft agar assays. The *bar graph* indicates the relative size of the colonies formed with the average size of control colonies arbitrarily set to 100%.

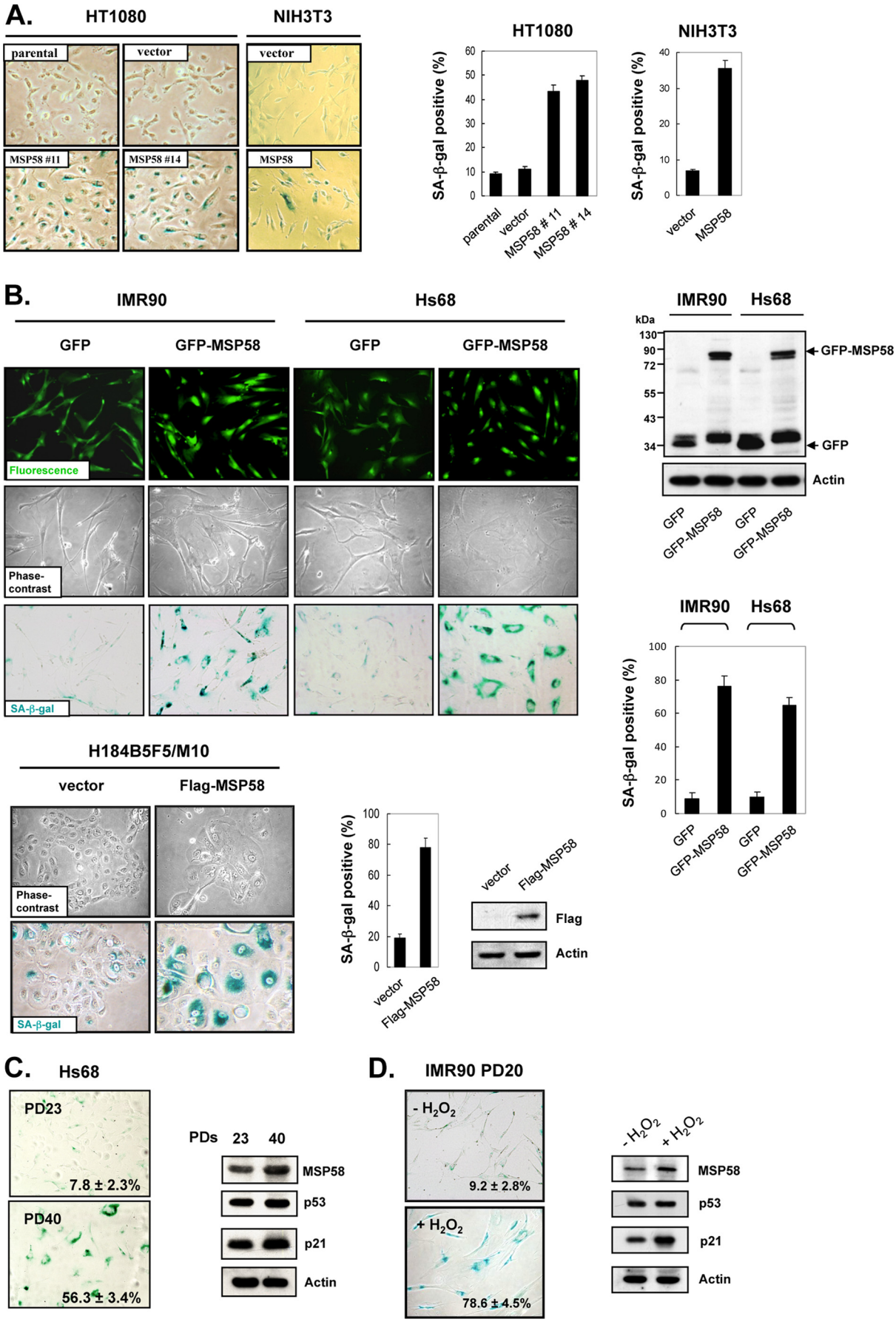
A.
HT1080
NIH3T3
parental
vector
vector
MSP58 #11
MSP58 #14
MSP58
HT1080
NIH3T3
SA-β-gal positive (%)
parental
vector
MSP58 # 11
MSP58 # 14
vector
MSP58
B.
IMR90
Hs68
GFP
GFP-MSP58
GFP
GFP-MSP58
Fluorescence
Phase-contrast
SA-β-gal
IMR90
Hs68
kDa
130
90
72
55
43
34
GFP-MSP58
GFP
Actin
GFP
GFP-MSP58
GFP
GFP-MSP58
IMR90
Hs68
SA-β-gal positive (%)
GFP
GFP-MSP58
GFP
GFP-MSP58
H184B5F5/M10
vector
Flag-MSP58
Phase-contrast
SA-β-gal
SA-β-gal positive (%)
vector
Flag-MSP58
vector
Flag-MSP58
Flag
Actin
C.
Hs68
PD23
7.8 ± 2.3%
PD40
56.3 ± 3.4%
PDs 23 40
MSP58
p53
p21
Actin
D.
IMR90 PD20
- H2O2
9.2 ± 2.8%
+ H2O2
78.6 ± 4.5%
- H2O2
+ H2O2
MSP58
p53
p21
Actin

si-3 and MSP58 si-5 efficiently knocked down MSP58 expression (supplemental Fig. S2). Depletion of the endogenous MSP58 protein in HeLa and HT1080 cells was further confirmed by Western blotting using the anti-MSP58 antibody (Fig. 1*A*). However, when we established stable MSP58 knockdown clones, cell death was induced during antibiotic selection in all cells expressing MSP58 si-3 or MSP58 si-5. MSP58-silenced cells displayed the typical morphological changes of apoptosis and showed an increase in the number of TUNEL-positive cells (Fig. 1, *B* and C). We further examined γ-tubulin immunostaining in MSP58-silenced cells and discovered a high proportion of multipolar spindle formation (Fig. 1*D*), which was consistent with a previous report (25). These studies suggested that MSP58 proteins are essential for normal cell division and viability.

Ectopic Expression of MSP58 Induces Context-dependent Roles in Controlling Cell Proliferation—We further established human fibrosarcoma HT1080 cell lines that exhibited stable expression of ectopic MSP58. Unexpectedly, several MSP58 clones, including clones 11 and 14, showed senescence-like phenotypes as typified by enlarged, flattened cells; accumulation of some binucleated cells; and a slower growth rate than that of parental or vector control cells (Fig. 2*A*). Similar morphological alterations and growth arrest were observed in stably MSP58-expressing NIH3T3 cells (Fig. 2*A*), notably HT1080 and NIH3T3 cells carrying the WT p53 and Rb alleles. To confirm that functional p53/Rb is required for MSP58-induced phenotypic changes, stable MSP58 cell lines were established in other cancer cells, including the A549 (lung adenocarcinoma), HCT116 (colon carcinoma), and U2OS (osteosarcoma) cell lines that express both WT p53 and Rb and the HeLa (cervical carcinoma; p53/Rb-defective), Saos-2 (osteosarcoma; p53/Rb-defective), and SW-13 (adrenocortical carcinoma; expressing mutant p53 but normal Rb) cell lines. Interestingly, MSP58 induced only partial abrogation of growth inhibition in U2OS cells, whereas A549 and HCT116 MSP58-overexpressing populations grew at rates similar to that of the control and exhibited a normal morphology (data not shown), suggesting that these cell lines lack functions other than p53 and Rb that are required for MSP58 to induce growth inhibition. In contrast, HeLa, Saos-2, and SW-13 cells with stable MSP58 overexpression proliferated more rapidly and exhibited no morphological differences compared with control cells (Fig. 2*B* and data not shown), suggesting the possibility that p53 plays a role in regulating the effects induced by MSP58. Consistently, HT1080 MSP58 clone 11 and 14 cells formed fewer colonies on monolayers and smaller colonies in soft agar. In contrast, HeLa, Saos-2, and SW-13 MSP58 cells exhibited marked colony formation in terms of both numbers and sizes (Fig. 2, *C* and *D*). These results revealed an unanticipated antiproliferative function of MSP58.

MSP58 Inhibits Growth by Cellular Senescence, and Replicative and Stress-induced Senescence Increases MSP58 Expression—To confirm that MSP58-overexpressing cells entered senescence, we analyzed DNA content using flow cytometry with propidium iodide staining. HT1080 MSP58 clone 11 and 14 cells showed decreased fractions in the G_1 phase resulting from cells accumulating in the S and G_2/M phases and elevated forward and side scatter relative to control cells, respectively reflecting increased cell size and granularity (supplemental Fig. S3). Additionally, these cells displayed a marked reduction in telomerase activity (supplemental Experimental Procedures, and Fig. S4). Notably, stable HT1080 and NIH3T3 transfectants expressing MSP58 showed elevated SA-β-gal activity, a classical biomarker of senescence (Fig. 3*A*). For further clarification of the effects of MSP58 in normal cells, we infected human diploid IMR90 and Hs68 fibroblasts with a retroviral vector encoding a GFP-MSP58 fusion or control vector. After selection, MSP58-infected cells displayed a large size with a flattened shape and significantly increased SA-β-gal activity compared with control cells (Fig. 3*B*). Similar results were observed for the normal human mammary epithelial H184B5F5/M10 cell line stably overexpressing MSP58 (Fig. 3*B*, *bottom panel*). Furthermore, we checked whether MSP58 expression increased during senescence. We found that MSP58 protein expression increased in later passages of IMR90 and Hs68 cells (Fig. 3*C* and data not shown). Moreover, MSP58 was up-regulated in IMR90 cells subjected to H_2O_2-induced premature senescence (Fig. 3*D*). These processes were accompanied by increased p53 and p21 expression levels. Altogether, these results indicate that MSP58 might be an important mediator of cellular senescence.

MSP58 Regulates Senescence through DNA Damage and p53/p21 Pathway—To obtain mechanistic insights, we examined protein levels of several cell cycle regulators implicated in senescence. As shown in Fig. 4*A*, higher p53 and p21 levels were observed in HT1080 MSP58 clone 11 and 14 cells compared with control cells and coincided with induction of p21 mRNA levels (Fig. 4*B*). Elevated levels of p53 and p21 proteins were also detected in MSP58-overexpressing IMR90, Hs68, and H184B5F5/M10 cells; however, p16 was not up-regulated (data not shown). Additionally, MSP58 induced the accumulation of hypophosphorylated Rb and reductions in total Rb, cyclin A, and cyclin E2 levels, whereas modest levels of cyclin B1 and cyclin D decreased. No significant alterations in cyclin E levels were found. Effects of MSP58 on the transcriptional activation of the p21 promoter and its dependence on p53 were further investigated. Luciferase reporter genes are driven by either the intact p21 promoter (WWP-Luc; p21-WT) or truncated p21 promoters in which one or two of the major p53-binding elements (*i.e.* p21-sm and p21-dm) are missing. Transcription of the WWP-Luc reporter was induced in both HT1080 MSP58 clone 11 and 14 cells (Fig. 4*B*). Cells transfected with the trun-

FIGURE 3. **Effects of MSP58 expression on cell senescence.** *A*, HT1080 and NIH3T3 parental, vector, and MSP58 stable clones were stained for SA-β-gal. At least 100 cells were scored from five randomly selected fields. *Columns*, mean percentage of positive cells; *bars*, S.D. *B*, IMR90 and Hs68 fibroblasts were infected with a retrovirus encoding GFP or GFP-MSP58. H184B5F5/M10 cells were stably transfected with the control vector or MSP58. After selection, cells were subjected to immunoblotting and microscopic analysis of green fluorescence, cell morphology, and SA-β-gal activity as in *A*. Images are all at the same magnification (200*x*). *C*, Hs68 fibroblasts at PD 23 (proliferating) and 40 (senescing) were stained for SA-β-Gal expression and quantified. Total cell lysates were analyzed using immunoblotting for MSP58, p53, p21, and actin. *D*, IMR90 cells at PD 20 were incubated with 500 μmol/liter hydrogen peroxide (H_2O_2) for 2 h of pretreatment and evaluated for SA-β-gal activity and subjected to immunoblotting analysis on day 5. *PD*, population doubling.

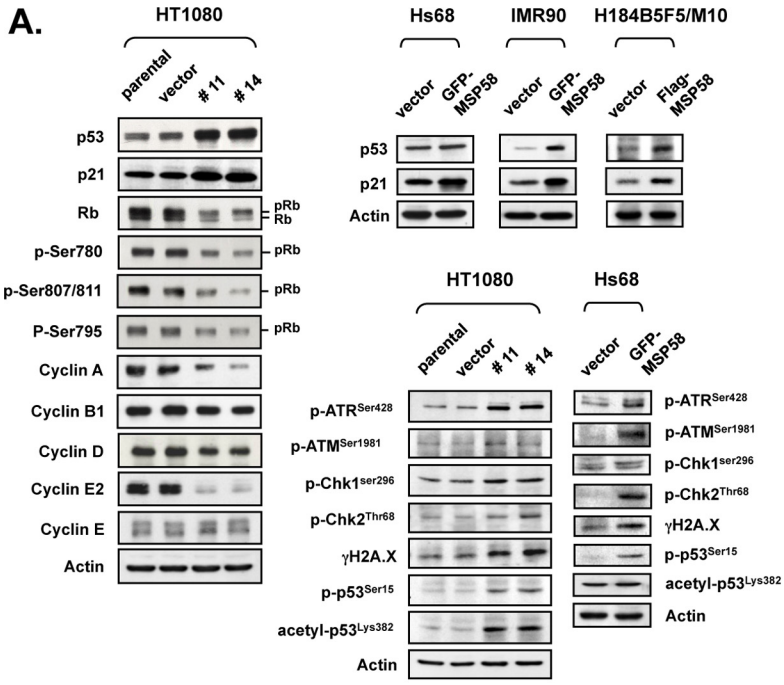
A.
HT1080
parental
vector
11
14
p53
p21
Rb
p-Ser780
p-Ser807/811
P-Ser795
Cyclin A
Cyclin B1
Cyclin D
Cyclin E2
Cyclin E
Actin
pRb
Hs68
IMR90
H184B5F5/M10
vector
GFP-MSP58
Flag-MSP58
p-ATR Ser428
p-ATM Ser1981
p-Chk1 ser296
p-Chk2 Thr68
γH2A.X
p-p53 Ser15
acetyl-p53 Lys382

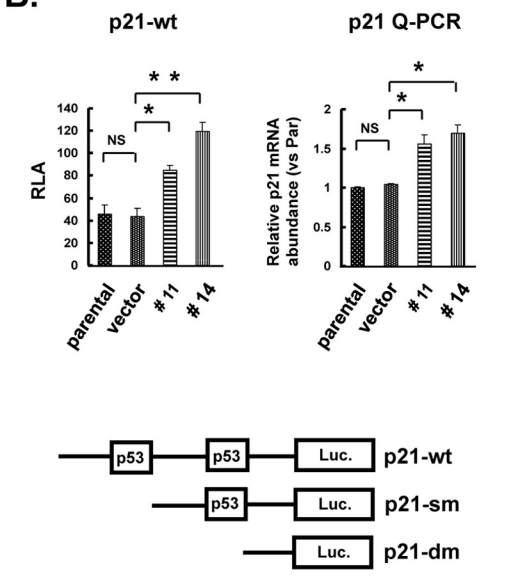
B.
p21-wt
p21 Q-PCR
RLA
Relative p21 mRNA abundance (vs Par)
NS
parental
vector
11
14
p53
Luc.
p21-wt
p21-sm
p21-dm
HT1080 vector
HT1080 MSP58 # 11

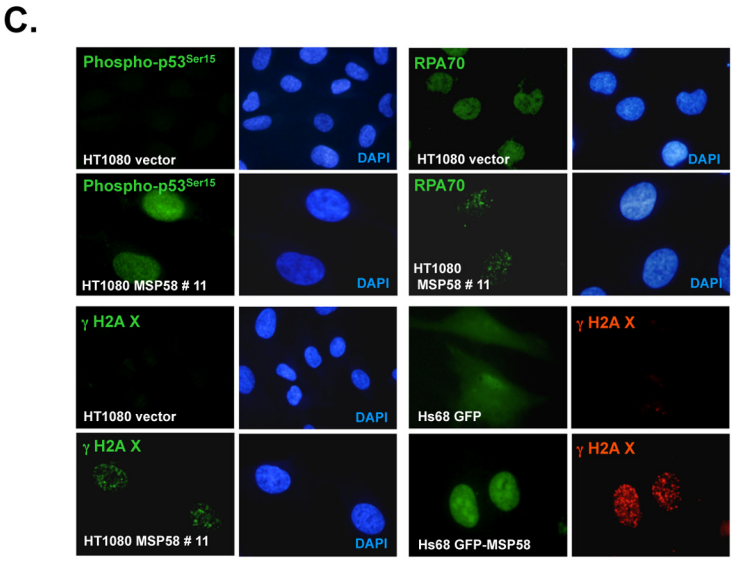
C.
Phospho-p53 Ser15
RPA70
DAPI
HT1080 vector
HT1080 MSP58 # 11
γ H2A X
Hs68 GFP
Hs68 GFP-MSP58

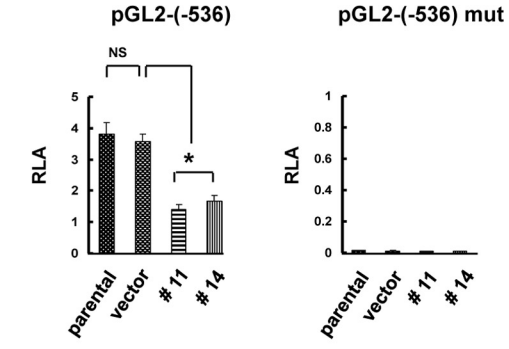
pGL2-(-536)
pGL2-(-536) mut
RLA
NS
parental
vector
11
14

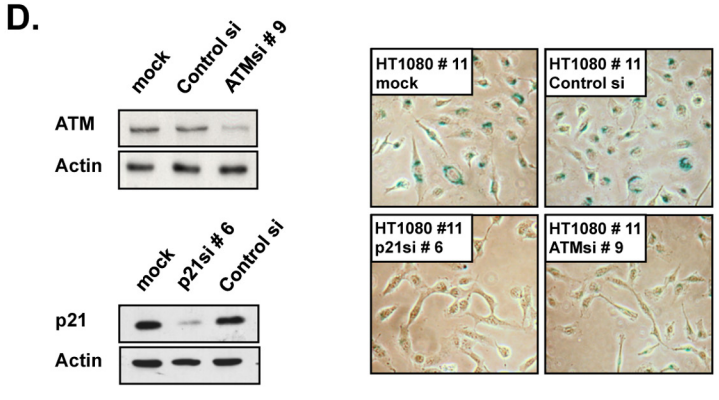
D.
mock
Control si
ATMsi # 9
ATM
Actin
p21si # 6
p21
HT1080 # 11 mock
HT1080 # 11 Control si
HT1080 #11 p21si # 6
HT1080 # 11 ATMsi # 9

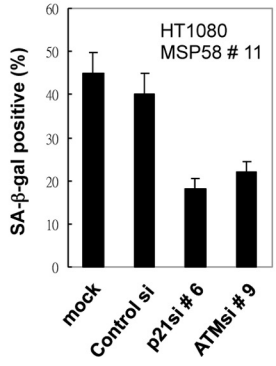
SA-β-gal positive (%)
HT1080 MSP58 # 11
mock
Control si
p21si # 6
ATMsi # 9

cated constructs showed substantially reduced responses as the p21-dm construct was not induced, indicating that MSP58 regulates p21 promoter activity through the p53 protein. Additionally, stable overexpression of MSP58 resulted in the inhibition of luciferase activity directed by the B-myb promoter (pGL2-(−536)), which contains a potential E2F-binding site, whereas there was no effect on the pGL2-(−536)mut. promoter. Furthermore, we observed that phosphorylated (Ser^{15}) and acetylated (Lys^{382}) p53 levels, phosphorylated forms of DNA damage-regulated kinases ATM/ATR and Chk1/Chk2, and phosphorylated histone H2AX (γ-H2AX) were elevated in MSP58-overexpressing HT1080 and Hs68 cells (Fig. 4*A*). Thus, MSP58 overexpression elicits a potent DNA damage response. Conversely, no alterations in phospho-ATM/ATR or phospho-Chk1/Chk2 expression levels were observed in HeLa, Saos-2, or SW-13 cells with stable MSP58 transfection (data not shown). The immunofluorescence analysis consistently revealed that the size of nuclear foci stained with RPA70 and γ-H2AX and the amount of nuclear phospho-$p53Ser^{15}$ were measurably greater in MSP58-overexpressing cells (Fig. 4*C*), suggesting replication stress and formation of DNA strand breaks. Furthermore, depletion of ATM or p21 using shRNA transfection significantly reduced the incidence of MSP58-induced senescent phenotypes as shown by the representative stable clones HT1080 MSP58 clone 11-ATMsi 9 and MSP58 clone 11-p21si6 (Fig. 4*D*). Consequently, the ATM-mediated DNA damage response-p53/p21 pathway is involved in MSP58-induced senescence.

Induction of Cellular Senescence by MSP58 through p53-dependent Pathway—To evaluate whether activation of the p53 pathway is essential for the induction of cellular senescence by MSP58, we utilized a sequence-specific RNA interference approach to knock down p53 levels in normal cells using a lentiviral delivery system. IMR90 and Hs68 cells were first transduced with shRNAs targeting p53 or luciferase and then infected with retrovirus carrying *MSP58* (Fig. 5*A*). The Western blot analysis demonstrated a dramatic loss of p53 protein in both endogenous and MSP58-activated p53 upon shRNA treatments (Fig. 5*B*). Significantly, down-regulation of p53 in cells expressing MSP58 resulted in increased cell growth and decreased β-galactosidase staining in both IMR90 and Hs68 cells (Fig. 5*C*), suggesting that suppression of p53 alleviates senescence induced by MSP58 in normal cells. To obtain more evidence on whether MSP58-induced senescence involves a p53 signaling pathway, we compared the effects of MSP58 up-regulation in $p53^{+/+}$ MEFs *versus* $p53^{-/-}$ MEFs. As in IMR90, Hs68, and NIH3T3 cells, transduction of MSP58 in $p53^{+/+}$ MEFs resulted in proliferative arrest within 3–4 days (Fig. 5*D*, *left panel*). In contrast, transduction of MSP58 in $p53^{-/-}$ MEFs strongly increased cell proliferation. As before, growth arrest was associated with cellular senescence because 46% of MEFs were β-galactosidase-positive after 8 days compared with 4% of the vector control (Fig. 5*D*, *right panel*). Elevated numbers of senescent cells were not observed in $p53^{-/-}$ MEFs, indicating that p53 is required for MSP58-induced senescence. Consistently, $p53^{+/+}$ MEFs displayed up-regulation of *p53* upon transduction of MSP58 (Fig. 5*E*). Not only did MSP58-transduced $p53^{-/-}$ MEFs show an enhanced proliferative potential, but they also exhibited an increased ability to form colonies on tissue culture plates compared with control transduced cells (Fig. 5*F*). Together, these results indicate that MSP58-induced cellular senescence is mediated through a p53-dependent pathway.

BRG1 Is Associated with MSP58 and Is Required for MSP58-induced Senescence—We previously isolated BRG1, the central catalytic ATPase of the SWI/SNF chromatin-remodeling apparatus, as a novel MSP58-interacting protein by yeast two-hybrid screening.[5] MSP58 selectively bound to the N-terminal domain (amino acids 1–750) of BRG1 (Fig. 6*A*). The N-terminal region of BRG1 contains a proline-rich domain, which is often implicated in protein-protein interactions (40). Overexpressed MSP58 and BRG1 proteins were reciprocally coimmunoprecipitated in COS-1 cells (Fig. 6*B*). Additionally, endogenous BRG1 and p53 proteins were coimmunoprecipitated with an anti-FLAG antibody in HT1080 MSP58 clone 11 cells. These results provide evidence that MSP58, BRG1, and p53 can form a complex in cells. Because MSP58 up-regulates p21 expression through p53 and BRG1 controls cellular senescence by up-regulating p21 (41), we were curious as to whether MSP58 and BRG1 were localized within transcriptional complexes on p53 cognate sites of the p21 promoter. Therefore, using a ChIP analysis, we showed the coexistence of MSP58 and BRG1 at two p53-binding sites (Fig. 6*C*, *upper left panel*, sites 1 and 2) but not on a region ~3 kb upstream of the transcription initiation site (site 3) of the p21 promoter. Furthermore, additional p53 and BRG1 proteins were detected on the p21 promoter in HT1080 MSP58 clone 11 and 14 cells compared with control cells (Fig. 6*C*, *upper right panel*). In contrast, no signals were detected in p53-null Saos-2 cells (Fig. 6*C*, *bottom panel*). A re-ChIP assay showed that p53 and BRG1 interacted with MSP58 at the p21 promoter (Fig. 6*C*, *middle panel*). These results suggest that activation of the p21 promoter by p53 is involved in recruiting both MSP58 and BRG1. To determine whether BRG1 is required for MSP58-induced senescence, we demonstrated that the stable BRG1 knockdown cell line HT1080 MSP58 clone 11-BRG1si4 partially reduced the incidence of MSP58-induced senescence (Fig. 6*D*), activation of the p21 promoter, and

[5] D.-Y. Lin and H.-M. Shih, unpublished data.

FIGURE 4. **MSP58 regulates senescence through DNA damage response-p53/p21 signaling pathway.** *A*, total cell extracts were analyzed using immunoblotting with the indicated antibodies. *B*, luciferase activities in HT1080 parental, vector, and/or MSP58 clone 11 and 14 cells transiently transfected with the p21 (p21-WT, p21-sm, or p21-dm) or B-myb (pGL2-(−536) or pGL2-(−536) mut.) luciferase reporter plasmid measured and normalized to *Renilla* luciferase activity. *Columns*, mean of three independent experiments; *bars*, S.D. *, $p < 0.05$; **, $p < 0.01$. *NS*, non-significant; *RLA*, relative luciferase activity. p21 mRNA expression was analyzed by quantitative RT-PCR using β-actin levels as the internal control. The expression of p21 in HT1080 parental cells was defined as 1.0, and other values were normalized accordingly. *C*, HT1080 vector or MSP58 clone 11 cells were immunostained for phospho-$p53Ser^{15}$, RPA70, and γ-H2AX (*green*). Nuclear DNA was stained with DAPI. Hs68 cells infected with the GFP vector or GFP-MSP58 were processed for GFP (*green*) fluorescence and γ-H2AX (*red*) immunostaining. *D*, generation of ATM- or p21-depleted cell lines. pSUPER empty vector (*mock*) or shRNAs against the control, ATM, or p21 were stably transfected into HT1080 MSP58 clone 11 cells. After selection, immunoblotting and SA-β-Gal staining were analyzed.

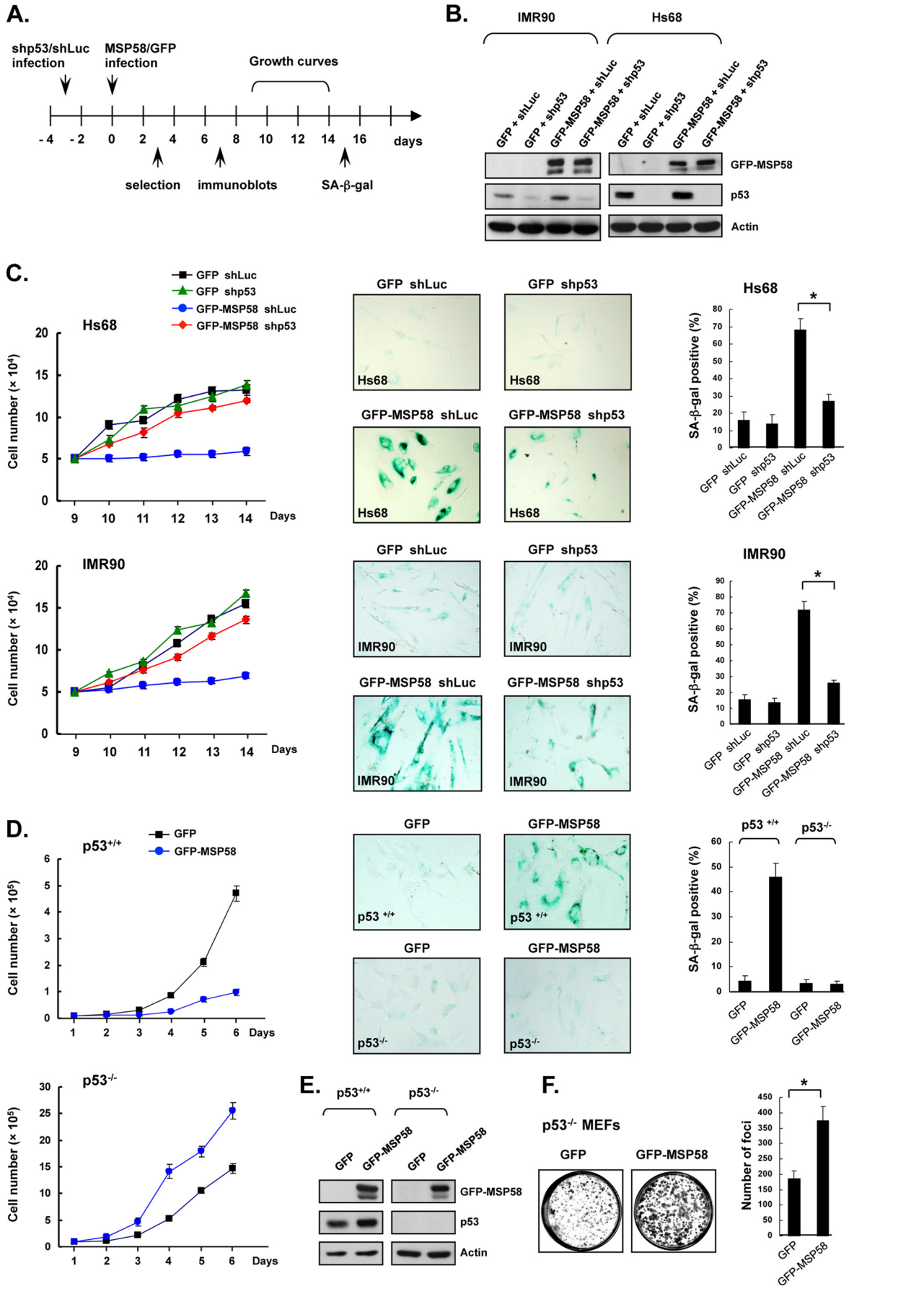
A.
shp53/shLuc infection
MSP58/GFP infection
Growth curves
-4 -2 0 2 4 6 8 10 12 14 16 days
selection
immunoblots
SA-β-gal
B.
IMR90
Hs68
GFP + shLuc
GFP + shp53
GFP-MSP58 + shLuc
GFP-MSP58 + shp53
GFP-MSP58
p53
Actin
C.
GFP shLuc
GFP shp53
GFP-MSP58 shLuc
GFP-MSP58 shp53
Hs68
Cell number (× 10⁴)
Days
IMR90
SA-β-gal positive (%)
D.
p53+/+
p53-/-
GFP
GFP-MSP58
Cell number (× 10⁵)
E.
F.
p53-/- MEFs
Number of foci

repression of E2F-medited transcription (Fig. 6*E*). Furthermore, overexpressing BRG1, but not MSP58, induced a flattened shape in SW-13 (BRG1-null) cells (Fig. 6*F*). These findings indicate that BRG1 is a critical mediator of MSP58-induced senescence and transcriptional regulation.

Differential Expression of MSP58 in Human Tumors—MSP58 is reported to be up-regulated in colorectal cancer tissues (29). However, whether the expression of MSP58 is elevated in other cancer types is poorly understood. To examine whether MSP58 is differentially expressed in certain normal and tumor tissues, MSP58 cDNA was labeled and hybridized to an array blot containing representative paired tumor/normal tissues from several different cancers (Cancer Profiling Array II, BD Biosciences Clontech) (Fig. 7*A*). MSP58 was frequently found to be up-regulated (in >80% of patients) in tumors derived from the lungs, uterus, cervix, and testes but also in tumor samples derived from the breasts, ovaries, colon, stomach, rectum, thyroid gland, and skin (in ~60% of patients). In contrast, in kidney, liver, and pancreas carcinomas of some patients, MSP58 was down-regulated compared with normal tissues (in ~60% of patients). We further detected MSP58 expression profiles at the protein level using a tissue microarray (US Biomax, catalogue number BCN962) by an IHC analysis. Notably, the stained antigen was located in both nuclei and the cytoplasm. By comparison with matched normal tissues, strong expression of the MSP58 protein was observed in only a few restricted cases of human tumors, including the esophagus, cervix, colon, and skin, whereas down-regulated MSP58 expression was observed in tumors from the stomach, liver, kidneys, and pancreas (Fig. 7*B* and supplemental Table S1). Although further investigation with a larger number of samples is necessary, the IHC staining data were consistent with the MSP58 mRNA expression profiles. This differential expression pattern suggests that MSP58 may function as a critical component of cellular transformation and oncogenesis.

DISCUSSION

MSP58 family proteins control a diverse range of cellular processes, including cell proliferation and transformation. This study provides the first evidence of the involvement of MSP58 in cellular senescence. Several discoveries were made. First, MSP58 protein levels were up-regulated in both replicative and stress-induced senescence, and ectopic overexpression of MSP58 triggered premature senescence in both normal and cancerous cells. Second, MSP58-induced senescence was associated with activation of the DNA damage response-p53/p21 signaling pathway. Third, MSP58 formed a complex with both p53 and BRG1, and MSP58-BRG1-p53 was associated with and transactivated the p21 promoter. Finally, MSP58 expression appeared to vary substantially between the tumor and matched normal tissues. This study provides links among MSP58, p53, and cellular senescence in human tumors and normal cells.

Our studies revealed that cell growth control by MSP58 may vary depending on the cellular context (Fig. 2). However, several studies indicated possible oncogenic activities of MSP58/TOJ3 in avian fibroblasts and PTEN-null MEFs (27, 28). That MSP58 can induce senescence in normal MEFs and normal human fibroblasts (this study) is puzzling because senescence is now recognized as a potent tumor-suppressive mechanism. In addition, forced expression of MCRS2 causes shortened telomeres in human hepatocellular carcinoma SMMC7721 cells, and MCRS2 can also inhibit telomerase activity *in vitro* (31). Telomere shortening and telomerase inhibition by MCRS2 seem contrary to MSP58/TOJ3 induction of cell transformation. Whether the reported effects of MCRS2 on telomerase/telomere regulation affect cell proliferation or induce senescence remains unclear. Our data also indicate that ectopic expression of MSP58 inhibits telomerase activity in HT1080 cells (supplemental Fig. S4). Moreover, we discovered that MSP58 protein levels increased during replicative senescence (Fig. 3*C*), and acute depletion of MSP58 expression caused apoptosis (Fig. 1). Consequently, we speculated that MSP58 can be protumorigenic in the context of aberrant genetic alterations associated with tumorigenesis and can suppress tumor progression by finely controlling senescence mechanisms in normal cells. However, the molecular mechanisms by which MSP58 exerts both its pro- and antioncogenic activities remain largely unclear.

We found that persistent MSP58 overexpression triggered a cellular senescence program by engaging ATR/ATM-mediated DNA damage signaling and the p53-dependent tumor suppressor pathway. 1) MSP58 induced high levels of p53 and its target p21 gene (Fig. 4*A*). 2) MSP58 activated p53-mediated transcription, increased the phosphorylated forms of ATM/ATR and Chk1/Chk2 kinases, and caused accumulation of γ-H2AX and RPA70 foci (Fig. 4, *A*–*C*). 3) RNA interference against ATM or p53 inhibited the MSP58-induced increase in SA-β-gal staining (Figs. 4*D* and 5*C*). 4) SA-β-gal staining by MSP58 overexpression increased in WT MEFs but not in $p53^{-/-}$ MEFs (Fig. 5*D*). Although the cellular transformation promoted by MSP58 was reported previously, induction of cellular senescence is a new observation. The dual roles of MSP58 in promoting transformation and senescence are not uncommon because they have been observed for many other oncogenes (42). The concept of oncogene-induced senescence recently emerged and possibly serves as a cell-autonomous barrier for cancer development (43–45). Pathways

FIGURE 5. **Induction of senescence in fibroblasts is dependent on p53.** *A*, experimental design. IMR90 and Hs68 cells were infected with shRNAs against p53 (*shp53*) or luciferase (*shLuc*) and then cultured at 37 °C for 3 days. Cells were then infected with a retroviruses carrying MSP58 or GFP. *B*, immunoblotting of IMR90 and Hs68 cells expressing luciferase (*Luc.*) control or p53 shRNA in combination with GFP control or MSP58. Cell extracts were prepared and analyzed by immunoblotting assays using antibodies against MSP58, p53, or actin. *C*, MSP58-expressing cells harboring shRNAs against p53 or luciferase were prepared as described above. Cell proliferation was measured by cell counting at the indicated times. SA-β-gal staining was performed on day 15 after the GFP or MSP58 infection. *Columns*, mean percentage of positive cells; *bars*, S.D. *D*, growth curves of $p53^{+/+}$ and $p53^{-/-}$ MEFs transduced as indicated were measured over a 6-day period. In a parallel experiment, MEFs were stained for SA-β-gal expression and quantified as in *C*. *E*, Western blots were performed to determine the protein abundance of GFP-MSP58 and p53 in wild-type and $p53^{-/-}$ MEFs transduced as indicated. *F*, focus formation assays. Microscopic images of $p53^{-/-}$ MEFs transduced as indicated after 10 days. Data represent the average number of foci ±S.D. from three independent experiments performed in triplicate. *, $p < 0.05$.

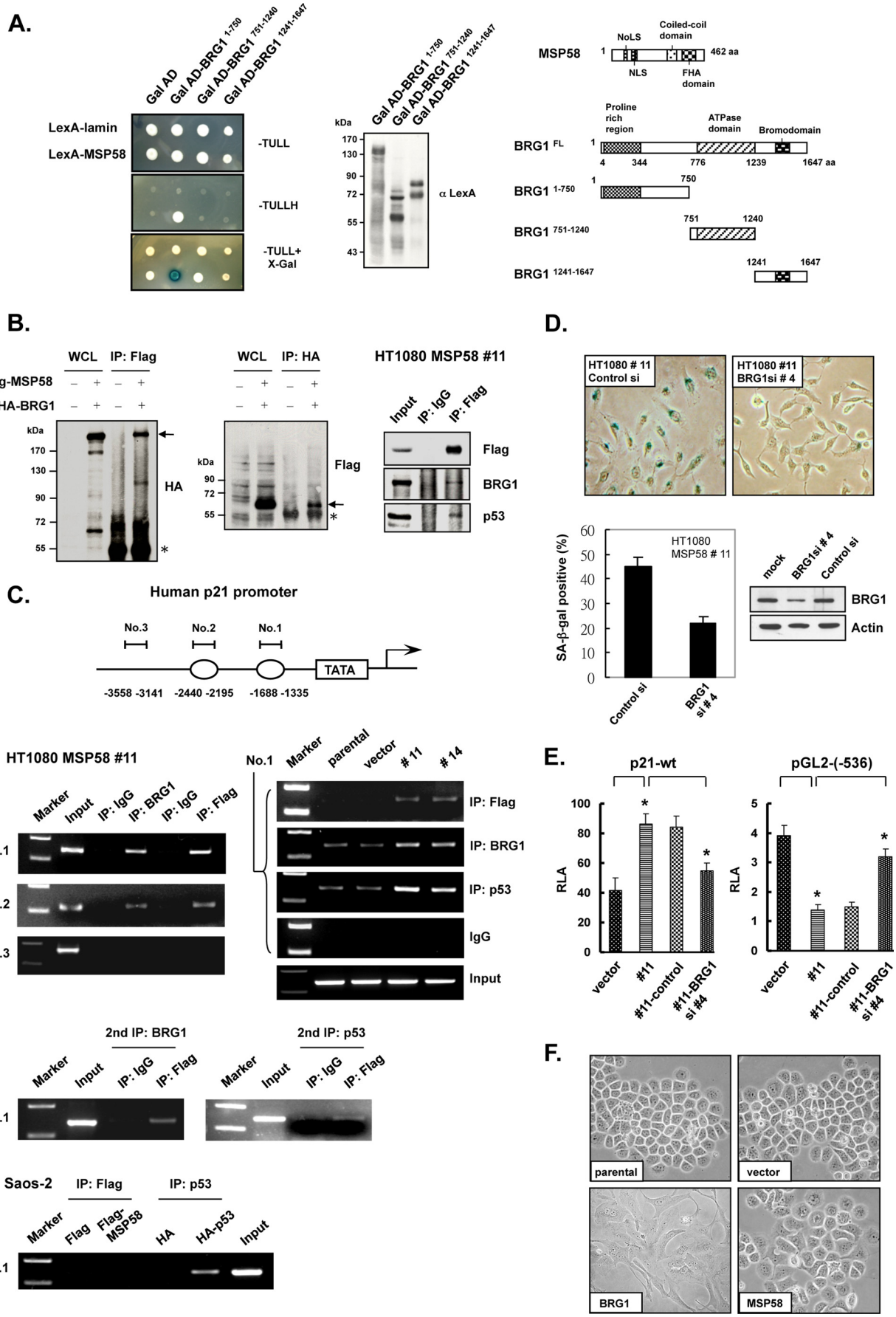
A.
Gal AD
Gal AD-BRG1 1-750
Gal AD-BRG1 751-1240
Gal AD-BRG1 1241-1647
LexA-lamin
LexA-MSP58
-TULL
-TULLH
-TULL+ X-Gal
kDa
170
130
90
72
55
43
α LexA
MSP58
NoLS
Coiled-coil domain
NLS
FHA domain
462 aa
BRG1 FL
Proline rich region
ATPase domain
Bromodomain
4
344
776
1239
1647 aa
BRG1 1-750
750
BRG1 751-1240
751
1240
BRG1 1241-1647
1241
1647
B.
WCL
IP: Flag
IP: HA
Flag-MSP58
HA-BRG1
HA
Flag
*
HT1080 MSP58 #11
Input
IP: IgG
IP: Flag
BRG1
p53
C.
Human p21 promoter
No.3
No.2
No.1
TATA
-3558 -3141
-2440 -2195
-1688 -1335
HT1080 MSP58 #11
Marker
Input
IP: IgG
IP: BRG1
IP: Flag
No.1
No.2
No.3
No.1
Marker
parental
vector
11
14
IP: Flag
IP: BRG1
IP: p53
IgG
Input
2nd IP: BRG1
2nd IP: p53
Saos-2
IP: Flag
IP: p53
Flag
Flag-MSP58
HA
HA-p53
D.
HT1080 # 11 Control si
HT1080 #11 BRG1si # 4
SA-β-gal positive (%)
HT1080 MSP58 # 11
Control si
BRG1 si # 4
mock
BRG1si # 4
Control si
BRG1
Actin
E.
p21-wt
pGL2-(-536)
RLA
vector
#11
#11-control
#11-BRG1 si #4
F.
parental
vector
BRG1
MSP58

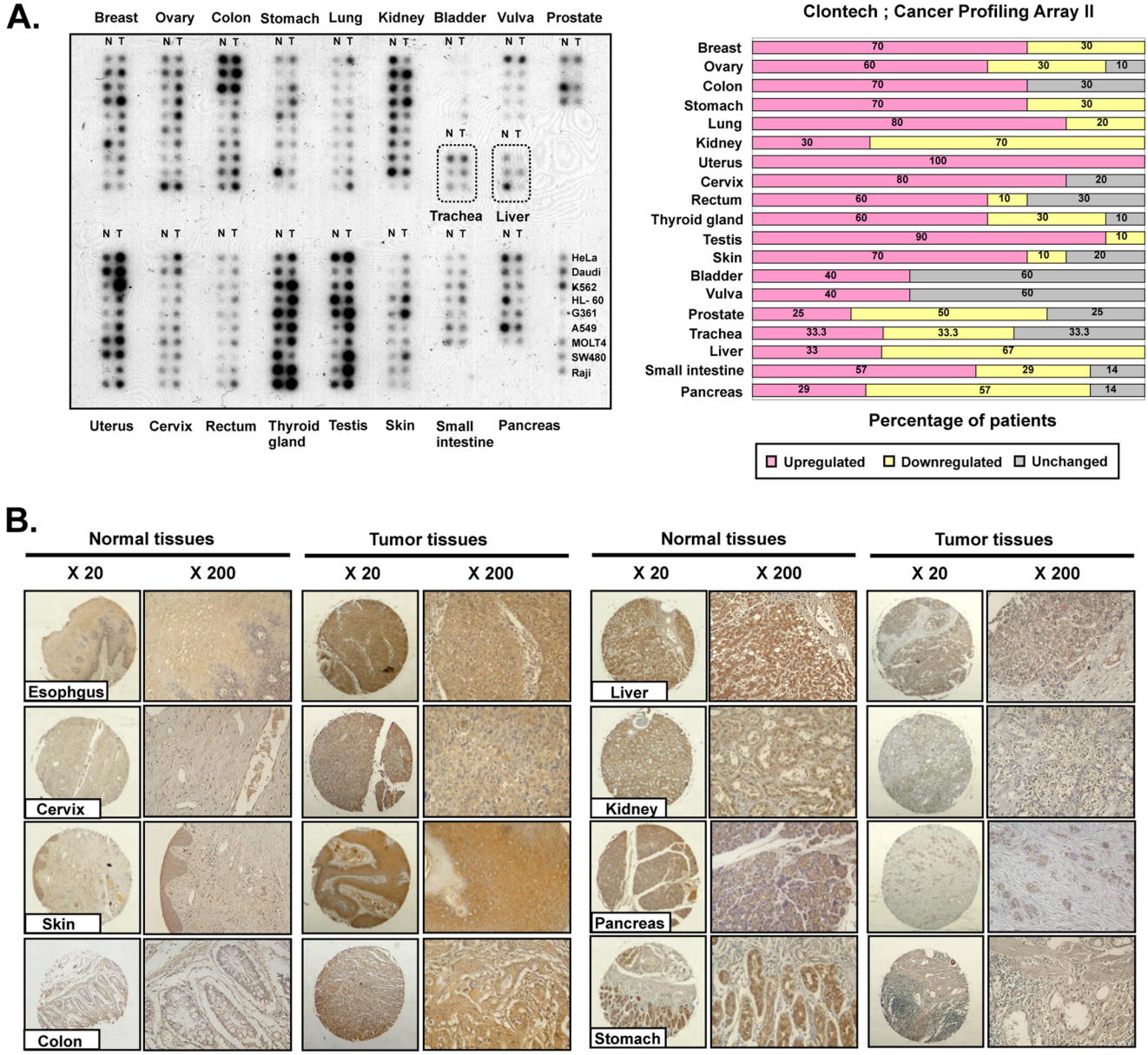

FIGURE 7. **MSP58 expression in paired normal/tumor tissues.** *A*, the Cancer Profiling Array II was hybridized with the ^{32}P-labeled full-length cDNA probe for MSP58. The intensity of the MSP58 probe signal was quantitated using a phosphorimaging system (Fujifilm BAS 2500) and normalized against ubiquitin. The *left panel* shows phosphorimage autoradiography. *N*, normal tissues; *T*, tumors. The *right panel* shows the fraction of tumors with MSP58 up-regulation as shown in *red*, down-regulation in *yellow*, and mRNA level retention or undetectable in *gray*. *B*, immunohistochemical staining of MSP58 protein expression in matched human tumors and normal counterparts by a tissue microarray. Images were analyzed using an Olympus AX70 light microscope with 20× and 200× *magnification*. Representative photographs show increased MSP58 expression in esophageal, cervical, skin, and colon tumors (*left panel*) with reduced expression in liver, kidney, pancreatic, and stomach tumors (*right panel*).

mediating oncogene-induced senescence have not been completely elucidated but seem to involve DNA replication stress and the eventual accumulation of DNA damage and activation of checkpoint control pathways, such as ATM/ATR, Chk kinases, and the downstream target p53 protein (46–49). Such an oncogene-driven DNA damage response

FIGURE 6. **BRG1 is involved in MSP58-mediated senescence.** *A*, interaction of MSP58 with BRG1 in a yeast two-hybrid assay. A schematic representation of BRG deletion mutants and MSP58 is depicted (*right*). *NLS*, nuclear-localization signal; *NoLS*, nucleolar-localization signal; *FHA*, forkhead-associated. A Western blot shows expression levels of BRG1 mutants in yeast cells (*middle*). Yeast transformants were spotted on histidine-containing (−*TULL*), without histidine (−*TULLH*), and X-Gal-containing (−*TULL* + *X-Gal*) media (*left*) in plates. LexA-lamin served as a negative control. *B*, coimmunoprecipitation assays. COS-1 cells were transfected with the indicated expression vectors. Whole cell lysates (*WCL*) from COS-1 and HT1080 MSP58 clone 11 were subjected to immunoprecipitation (*IP*) experiments followed by Western blot analysis with the indicated antibodies. *Arrows* indicate the positions of HA-BRG1 and FLAG-MSP58, whereas *stars* indicate the heavy chain of IgG. *C*, MSP58 forms a complex with both p53 and BRG1 on the p21 promoter. A schematic of the human p21 promoter showing the positions of the PCR primers of the p53-binding sites (*No.1* and *No.2*) and a control site (*No.3*) used for the ChIP assays. ChIP or re-ChIP was performed with the indicated cell lines, antibodies, and primer positions. *IgG*, control antibody. As a positive control, Saos-2 cells were transiently transfected with the HA-p53 construct. *D*, generation of stable cell lines with BRG1 depletion. Experiments were performed as in Fig. 4*D*. *E*, luciferase assay of the HT1080 vector or MSP58-overexpressing (*#11*), stable knockdown of BRG1 (*#11-BRG1 si #4*), or pSUPER control (*#11-control*) cells transiently transfected with the p21 or B-myb promoter-luciferase plasmid. *Columns*, mean; *bars*, S.D. *, $p < 0.05$. *F*, phase-contrast images of parental SW-13 and cells stably expressing the vector, BRG1, or MSP58. *WCL*, whole cell lysate; *RLA*, relative luciferase activity; *FHA*, forkhead-associated domain; *aa*, amino acids; *NLS*, nuclear localization signal; *NoLS*, nucleolar localization signal.

initiates and maintains senescence growth arrest to restrict the continued growth of malignant transformation in the early stages, thereby maintaining the tumor in a premalignant state. Our data suggest that MSP58-driven senescence closely resembles oncogene-induced senescence.

We conducted yeast two-hybrid screening using MSP58 as bait and identified several interacting partners. In addition to BRG1, nuclear factor related to κB-binding protein, is another candidate protein (data not shown). BRG1, a subunit of the SWI/SNF chromatin-remodeling complex, uses energy derived from ATP hydrolysis to alter the chromatin architecture of target promoters. ATP-dependent chromatin-remodeling complexes are divided into five major classes: SWI/SNF, NuRD/Mi-2/CHD, ISWI, INO80, and SWR1. MSP58 can form a complex with Mi-2β (a component of the NuRD complex), which up-regulates ribosomal gene transcription (22). Recently, MCRS2 was purified as part of a complex containing the histone acetyltransferase males absent on first (MOF) in both humans and flies (50). Independent studies by Conaway and co-workers (51) identified a collection of subunit compositions of human INO80-related chromatin-remodeling complexes; these proteins include nuclear factor related to κB-binding protein and MSP58. They also reported that the MSP58 protein is a component of the nonspecific lethal complex, which refers to additional MOF-containing histone acetyltransferase complexes (52). Therefore, the association of MSP58 with multiple chromatin-remodeling complexes suggests that MSP58 is critical for transcriptional modulation.

Previous studies strongly indicated that BRG1 possesses tumor-suppressive functions. The formation of flat, growth-arrested cells is induced by BRG1 by binding to Rb and the p53 protein (41, 53, 54). Additionally, BRG1 promotes p53-dependent transcription (55) and induction of p21 expression by associating with the p21 promoter (41, 56) while functioning as a co-repressor of E2F-targeted gene transcription by associating with Rb (57). This study proposes MSP58-induced senescence to be associated with p21 gene activation through two mechanisms. First, aberrant activation of MSP58 leads to the accumulation of replication-associated DNA damage and/or deregulation of telomerase/telomere control, which elicits activation of the DNA damage response, culminating in p53 activation and up-regulation of p21. Second, a transcription complex consisting of MSP58 and BRG1 cooperates with p53 to regulate the transcription of the p21 promoter. Moreover, MSP58 might also act as a transcriptional repressor of E2F target genes by associating with BRG1. We demonstrated that MSP58 overexpression suppresses E2F-mediated promoter activity and the levels of target genes, such as cyclins A and E2 (Fig. 4, *A* and *B*). Importantly, BRG1 knockdown abrogated MSP58-induced senescence and transcription modulation (Fig. 6, *D* and *E*). Overall, these results show the cooperative role of BRG1 in MSP58-mediated senescence.

The cancer profiling array blot results showed that MSP58 expression increased in various tumors (Fig. 7*A*), suggesting that MSP58 may play a fundamental oncogenic role in multiple body organs. Reduced expression or the absence of MSP58 was specifically observed in the liver, kidney, and pancreatic tumor tissues compared with their normal counterparts. The restricted pattern of expression suggests that MSP58 may be a diagnostic biomarker for a broad range of human cancers. Differential patterns of MSP58 expression in selected tumor tissues are consistent with most individual oncogenes (58). However, because MSP58 was identified as a senescence-associated gene involved in the endogenous replicative and exogenous stress-induced senescence program (Fig. 3, *C* and *D*), it is reasonable to speculate that the loss or down-regulated expression of MSP58 in the early stages of tumorigenesis might enable cells to bypass senescence and become immortalized after accumulating genetic alterations. This down-regulated or absent expression of MSP58 in tumors implies a protective role for MSP58 against tumorigenesis. Hence, whether MSP58 can function as a tumor suppressor remains unclear. MSP58 may act as an antitumorigenic molecule when bound to the tumor suppressors p53 and BRG1 and/or when connected to telomerase/telomere modulation. Because of the functional role of MSP58 in regulating cell proliferation and transcription, the current investigation, in accordance with previous studies, suggests additional levels of regulation of MSP58 functions in cancer progression in cell and tissue context-dependent manners. Further studies should clarify the factors that modulate MSP58 expression in normal cells and during tumorigenicity and how genetic mutations in cancer cells abrogate the tumor-suppressive functions of MSP58. In conclusion, this study provides valuable references for further investigations on the significance of MSP58 under physiological and pathophysiological conditions.

Acknowledgments—We thank Drs. Stephen P. Goff, Weei-Chin Lin, Roger J. Watson, Axel H. Schönthal, and Shih-Ming Huang for the plasmids; Dr. Fung-Fang Wang for providing the wild-type and p53-null (MEF) cells; Dr. Hsiu-Ming Shih for the yeast two-hybrid screening; Ping-Chieh Pao for assistance with the retroviral infection protocol; and Ching-Jan (Chris) Yu for the synthetic peptide design. We extend our gratitude to Drs. Tsung-Ping Su, Ming-Derg Lai, Ju-Ming Wang, Chi-Wu Chiang, Joseph T. Tseng, Chiou-Feng Lin, Yu-Liang Kuo, Kuen-Jer Tsai, Tsung-I Hsu, and Chiung-Yuan Ko for helpful discussions and Dan Chamberlin for English editing. The shRNA lentiviral vectors were obtained from the National RNAi Core Facility (The Institute of Molecular Biology/Genomic Research Center, Academia Sinica, Taiwan).

REFERENCES

1. Hayflick, L., and Moorhead, P. S. (1961) The serial cultivation of human diploid cell strains. *Exp. Cell Res.* **25,** 585–621
2. Blackburn, E. H. (2000) Telomere states and cell fates. *Nature* **408,** 53–56
3. Kim Sh, S. H., Kaminker, P., and Campisi, J. (2002) Telomeres, aging and cancer: in search of a happy ending. *Oncogene* **21,** 503–511
4. Stewart, S. A., and Weinberg, R. A. (2000) Telomerase and human tumorigenesis. *Semin. Cancer Biol.* **10,** 399–406
5. Chen, Q. M. (2000) Replicative senescence and oxidant-induced premature senescence. Beyond the control of cell cycle checkpoints. *Ann. N.Y. Acad. Sci.* **908,** 111–125
6. Ben-Porath, I., and Weinberg, R. A. (2005) The signals and pathways activating cellular senescence. *Int. J. Biochem. Cell Biol.* **37,** 961–976
7. Serrano, M., and Blasco, M. A. (2001) Putting the stress on senescence. *Curr. Opin. Cell Biol.* **13,** 748–753
8. Serrano, M., Lin, A. W., McCurrach, M. E., Beach, D., and Lowe, S. W. (1997) Oncogenic ras provokes premature cell senescence associated with accumulation of p53 and p16INK4a. *Cell* **88,** 593–602

9. Sitte, N., Merker, K., Von Zglinicki, T., Grune, T., and Davies, K. J. (2000) Protein oxidation and degradation during cellular senescence of human BJ fibroblasts: part I—effects of proliferative senescence. *FASEB J.* **14,** 2495–2502
10. Campisi, J. (2000) Cancer, aging and cellular senescence. *In Vivo* **14,** 183–188
11. Dimri, G. P., Lee, X., Basile, G., Acosta, M., Scott, G., Roskelley, C., Medrano, E. E., Linskens, M., Rubelj, I., and Pereira-Smith, O. (1995) A biomarker that identifies senescent human cells in culture and in aging skin *in vivo*. *Proc. Natl. Acad. Sci. U.S.A.* **92,** 9363–9367
12. Shay, J. W., Pereira-Smith, O. M., and Wright, W. E. (1991) A role for both RB and p53 in the regulation of human cellular senescence. *Exp. Cell Res.* **196,** 33–39
13. Hunter, T. (1993) Braking the cycle. *Cell* **75,** 839–841
14. Harper, J. W., Adami, G. R., Wei, N., Keyomarsi, K., and Elledge, S. J. (1993) The p21 Cdk-interacting protein Cip1 is a potent inhibitor of G1 cyclin-dependent kinases. *Cell* **75,** 805–816
15. Narita, M., Nũnez, S., Heard, E., Lin, A. W., Hearn, S. A., Spector, D. L., Hannon, G. J., and Lowe, S. W. (2003) Rb-mediated heterochromatin formation and silencing of E2F target genes during cellular senescence. *Cell* **113,** 703–716
16. Adams, P. D. (2007) Remodeling of chromatin structure in senescent cells and its potential impact on tumor suppression and aging. *Gene* **397,** 84–93
17. Braig, M., Lee, S., Loddenkemper, C., Rudolph, C., Peters, A. H., Schlegelberger, B., Stein, H., Dörken, B., Jenuwein, T., and Schmitt, C. A. (2005) Oncogene-induced senescence as an initial barrier in lymphoma development. *Nature* **436,** 660–665
18. Chen, Z., Trotman, L. C., Shaffer, D., Lin, H. K., Dotan, Z. A., Niki, M., Koutcher, J. A., Scher, H. I., Ludwig, T., Gerald, W., Cordon-Cardo, C., and Pandolfi, P. P. (2005) Crucial role of p53-dependent cellular senescence in suppression of Pten-deficient tumorigenesis. *Nature* **436,** 725–730
19. Ivanova, A. V., Ivanov, S. V., and Lerman, M. L. (2005) Association, mutual stabilization, and transcriptional activity of the STRA13 and MSP58 proteins. *Cell. Mol. Life Sci.* **62,** 471–484
20. Lin, D. Y., and Shih, H. M. (2002) Essential role of the 58-kDa microspherule protein in the modulation of Daxx-dependent transcriptional repression as revealed by nucleolar sequestration. *J. Biol. Chem.* **277,** 25446–25456
21. Ren, Y., Busch, R. K., Perlaky, L., and Busch, H. (1998) The 58-kDa microspherule protein (MSP58), a nucleolar protein, interacts with nucleolar protein p120. *Eur. J. Biochem.* **253,** 734–742
22. Shimono, K., Shimono, Y., Shimokata, K., Ishiguro, N., and Takahashi, M. (2005) Microspherule protein 1, Mi-2β, and RET finger protein associate in the nucleolus and up-regulate ribosomal gene transcription. *J. Biol. Chem.* **280,** 39436–39447
23. Wu, J. L., Lin, Y. S., Yang, C. C., Lin, Y. J., Wu, S. F., Lin, Y. T., and Huang, C. F. (2009) MCRS2 represses the transactivation activities of Nrf1. *BMC Cell Biol.* **10,** 9
24. Andersen, D. S., Raja, S. J., Colombani, J., Shaw, R. L., Langton, P. F., Akhtar, A., and Tapon, N. (2010) *Drosophila* MCRS2 associates with RNA polymerase II complexes to regulate transcription. *Mol. Cell. Biol.* **30,** 4744–4755
25. Hirohashi, Y., Wang, Q., Liu, Q., Du, X., Zhang, H., Sato, N., and Greene, M. I. (2006) p78/MCRS1 forms a complex with centrosomal protein Nde1 and is essential for cell viability. *Oncogene* **25,** 4937–4946
26. Du, X., Wang, Q., Hirohashi, Y., and Greene, M. I. (2006) DIPA, which can localize to the centrosome, associates with p78/MCRS1/MSP58 and acts as a repressor of gene transcription. *Exp. Mol. Pathol.* **81,** 184–190
27. Bader, A. G., Schneider, M. L., Bister, K., and Hartl, M. (2001) TOJ3, a target of the v-Jun transcription factor, encodes a protein with transforming activity related to human microspherule protein 1 (MCRS1). *Oncogene* **20,** 7524–7535
28. Okumura, K., Zhao, M., Depinho, R. A., Furnari, F. B., and Cavenee, W. K. (2005) Cellular transformation by the MSP58 oncogene is inhibited by its physical interaction with the PTEN tumor suppressor. *Proc. Natl. Acad. Sci. U.S.A.* **102,** 2703–2706
29. Shi, H., Chen, S., Jin, H., Xu, C., Dong, G., Zhao, Q., Wang, W., Zhang, H., Lin, W., Zhang, J., Davidovic, L., Yao, L., and Fan, D. (2009) Downregulation of MSP58 inhibits growth of human colorectal cancer cells via regulation of the cyclin D1-cyclin-dependent kinase 4-p21 pathway. *Cancer Sci.* **100,** 1585–1590
30. Lin, W., Zhang, J., Zhang, J., Liu, X., Fei, Z., Li, X., Davidovic, L., Tang, Z., Shen, L., Deng, Y., Yang, A., Han, H., Zhang, X., and Yao, L. (2009) RNAi-mediated inhibition of MSP58 decreases tumour growth, migration and invasion in a human glioma cell line. *J. Cell. Mol. Med.* **13,** 4608–4622
31. Song, H., Li, Y., Chen, G., Xing, Z., Zhao, J., Yokoyama, K. K., Li, T., and Zhao, M. (2004) Human MCRS2, a cell-cycle-dependent protein, associates with LPTS/PinX1 and reduces the telomere length. *Biochem. Biophys. Res. Commun.* **316,** 1116–1123
32. Lam, E. W., and Watson, R. J. (1993) An E2F-binding site mediates cell-cycle regulated repression of mouse B-myb transcription. *EMBO J.* **12,** 2705–2713
33. Wu, R. C., and Schönthal, A. H. (1997) Activation of p53-p21waf1 pathway in response to disruption of cell-matrix interactions. *J. Biol. Chem.* **272,** 29091–29098
34. McCabe, N., Turner, N. C., Lord, C. J., Kluzek, K., Bialkowska, A., Swift, S., Giavara, S., O'Connor, M. J., Tutt, A. N., Zdzienicka, M. Z., Smith, G. C., and Ashworth, A. (2006) Deficiency in the repair of DNA damage by homologous recombination and sensitivity to poly(ADP-ribose) polymerase inhibition. *Cancer Res.* **66,** 8109–8115
35. Shats, I., Milyavsky, M., Tang, X., Stambolsky, P., Erez, N., Brosh, R., Kogan, I., Braunstein, I., Tzukerman, M., Ginsberg, D., and Rotter, V. (2004) p53-dependent down-regulation of telomerase is mediated by p21waf1. *J. Biol. Chem.* **279,** 50976–50985
36. Zhang, J., Ohta, T., Maruyama, A., Hosoya, T., Nishikawa, K., Maher, J. M., Shibahara, S., Itoh, K., and Yamamoto, M. (2006) BRG1 interacts with Nrf2 to selectively mediate HO-1 induction in response to oxidative stress. *Mol. Cell. Biol.* **26,** 7942–7952
37. Lin, D. Y., Fang, H. I., Ma, A. H., Huang, Y. S., Pu, Y. S., Jenster, G., Kung, H. J., and Shih, H. M. (2004) Negative modulation of androgen receptor transcriptional activity by Daxx. *Mol. Cell. Biol.* **24,** 10529–10541
38. Dignam, J. D., Lebovitz, R. M., and Roeder, R. G. (1983) Accurate transcription initiation by RNA polymerase II in a soluble extract from isolated mammalian nuclei. *Nucleic Acids Res.* **11,** 1475–1489
39. Chen, C. H., Lu, P. J., Chen, Y. C., Fu, S. L., Wu, K. J., Tsou, A. P., Lee, Y. C., Lin, T. C., Hsu, S. L., Lin, W. J., Huang, C. Y., and Chou, C. K. (2007) FLJ10540-elicited cell transformation is through the activation of PI3-kinase/AKT pathway. *Oncogene* **26,** 4272–4283
40. Kadam, S., and Emerson, B. M. (2003) Transcriptional specificity of human SWI/SNF BRG1 and BRM chromatin remodeling complexes. *Mol. Cell* **11,** 377–389
41. Kang, H., Cui, K., and Zhao, K. (2004) BRG1 controls the activity of the retinoblastoma protein via regulation of p21CIP1/WAF1/SDI. *Mol. Cell. Biol.* **24,** 1188–1199
42. Sharma, S. V., and Settleman, J. (2010) Exploiting the balance between life and death: targeted cancer therapy and "oncogenic shock". *Biochem. Pharmacol.* **80,** 666–673
43. Courtois-Cox, S., Jones, S. L., and Cichowski, K. (2008) Many roads lead to oncogene-induced senescence. *Oncogene* **27,** 2801–2809
44. Halazonetis, T. D., Gorgoulis, V. G., and Bartek, J. (2008) An oncogene-induced DNA damage model for cancer development. *Science* **319,** 1352–1355
45. Prieur, A., and Peeper, D. S. (2008) Cellular senescence *in vivo*: a barrier to tumorigenesis. *Curr. Opin. Cell Biol.* **20,** 150–155
46. Bartkova, J., Horejsí, Z., Koed, K., Krämer, A., Tort, F., Zieger, K., Guldberg, P., Sehested, M., Nesland, J. M., Lukas, C., Ørntoft, T., Lukas, J., and Bartek, J. (2005) DNA damage response as a candidate anti-cancer barrier in early human tumorigenesis. *Nature* **434,** 864–870
47. Bartkova, J., Rezaei, N., Liontos, M., Karakaidos, P., Kletsas, D., Issaeva, N., Vassiliou, L. V., Kolettas, E., Niforou, K., Zoumpourlis, V. C., Takaoka, M., Nakagawa, H., Tort, F., Fugger, K., Johansson, F., Sehested, M., Andersen, C. L., Dyrskjot, L., Ørntoft, T., Lukas, J., Kittas, C., Helleday, T., Halazonetis, T. D., Bartek, J., and Gorgoulis, V. G. (2006) Oncogene-induced senescence is part of the tumorigenesis barrier imposed by DNA damage check-

points. *Nature* **444,** 633–637
48. Di Micco, R., Fumagalli, M., Cicalese, A., Piccinin, S., Gasparini, P., Luise, C., Schurra, C., Garre', M., Nuciforo, P. G., Bensimon, A., Maestro, R., Pelicci, P. G., and d'Adda di Fagagna, F. (2006) Oncogene-induced senescence is a DNA damage response triggered by DNA hyper-replication. *Nature* **444,** 638–642
49. Mallette, F. A., Gaumont-Leclerc, M. F., and Ferbeyre, G. (2007) The DNA damage signaling pathway is a critical mediator of oncogene-induced senescence. *Genes Dev.* **21,** 43–48
50. Raja, S. J., Charapitsa, I., Conrad, T., Vaquerizas, J. M., Gebhardt, P., Holz, H., Kadlec, J., Fraterman, S., Luscombe, N. M., and Akhtar, A. (2010) The nonspecific lethal complex is a transcriptional regulator in *Drosophila*. *Mol. Cell* **38,** 827–841
51. Chen, L., Cai, Y., Jin, J., Florens, L., Swanson, S. K., Washburn, M. P., Conaway, J. W., and Conaway, R. C. (2011) Subunit organization of the human INO80 chromatin remodeling complex: an evolutionarily conserved core complex catalyzes ATP-dependent nucleosome remodeling. *J. Biol. Chem.* **286,** 11283–11289
52. Cai, Y., Jin, J., Swanson, S. K., Cole, M. D., Choi, S. H., Florens, L., Washburn, M. P., Conaway, J. W., and Conaway, R. C. (2010) Subunit composition and substrate specificity of a MOF-containing histone acetyltransferase distinct from the male-specific lethal (MSL) complex. *J. Biol. Chem.* **285,** 4268–4272
53. Dunaief, J. L., Strober, B. E., Guha, S., Khavari, P. A., Alin, K., Luban, J., Begemann, M., Crabtree, G. R., and Goff, S. P. (1994) The retinoblastoma protein and BRG1 form a complex and cooperate to induce cell cycle arrest. *Cell* **79,** 119–130
54. Lee, D., Kim, J. W., Seo, T., Hwang, S. G., Choi, E. J., and Choe, J. (2002) SWI/SNF complex interacts with tumor suppressor p53 and is necessary for the activation of p53-mediated transcription. *J. Biol. Chem.* **277,** 22330–22337
55. Xu, Y., Zhang, J., and Chen, X. (2007) The activity of p53 is differentially regulated by Brm- and Brg1-containing SWI/SNF chromatin remodeling complexes. *J. Biol. Chem.* **282,** 37429–37435
56. Hendricks, K. B., Shanahan, F., and Lees, E. (2004) Role for BRG1 in cell cycle control and tumor suppression. *Mol. Cell. Biol.* **24,** 362–376
57. Zhang, H. S., Gavin, M., Dahiya, A., Postigo, A. A., Ma, D., Luo, R. X., Harbour, J. W., and Dean, D. C. (2000) Exit from G_1 and S phase of the cell cycle is regulated by repressor complexes containing HDAC-Rb-hSWI/SNF and Rb-hSWI/SNF. *Cell* **101,** 79–89
58. Chung, C. H., Bernard, P. S., and Perou, C. M. (2002) Molecular portraits and the family tree of cancer. *Nat. Genet.* **32,** (suppl.) 533–540